Hindawi
Advances in Civil Engineering
Volume 2023, Article ID 3754079, 16 pages
https://doi.org/10.1155/2023/3754079

Research Article

Investigation on Mining-Induced Floor Water Inrush from Column and Its Control Based on Microseismic Monitoring

Run Liu,[1,2] Guojun Zhi,[1] Shilei Yang,[1] and Xiaowei Xu[2]

[1]*Wanli No. 1 Coal Mine, Shenhua Baotou Energy Company with Limited Liability, Eerduosi 017000, Neimenggu, China*
[2]*School of Mechanics and Civil Engineering, University of Mining and Technology, Beijing 100083, China*

Correspondence should be addressed to Xiaowei Xu; xxw@student.cumtb.edu.cn

Received 27 August 2022; Revised 14 December 2022; Accepted 15 April 2023; Published 20 May 2023

Academic Editor: Guang-Liang Feng

Water inrush is the biggest threat for safe mining in the Ruifeng coalmine, located in North China. In the study mining area, the floor water inrush is mainly caused by mining activities and collapse column. In this article, the mechanical criteria of floor water inrush are obtained based on cusp catastrophe theory, which is used to assess floor water inrush risk in the Ruifeng coalmine. Theoretical analysis shows that floor water inrush is very likely to occur during coal mining without the influence of geological structures. Additionally, FLAC^{3D} was used to simulate the damage of floor strata during the mining face advances. Numerical results show that the water inrush channel occurs in front of the mining face due to the influence of stress concentration. Therefore, a microseismic monitoring system was applied to monitor the formation of water inrush pathway. Field monitoring results show that two water inrush pathways were accurately predicted and positioned. Based on the microseismic monitoring results, target grouting was adopted to prevent water inrush. This study provides significant guidance for the prevention of floor water inrush.

1. Introduction

Most coalmines located in the Permo-Carboniferous coalfields in North China are threatened by the Ordovician limestone aquifer under the coal seams [1–3]. The Ordovician limestone strata are confined aquifer containing a large amount of water with a high hydraulic pressure [4]. The floor strata between the confined aquifer and the coal seam, normally comprising mixed impermeable clay layers with high strength sandstone or carbonate layers, can serve as the water-resisting strata that prevent the upward migration of confined water. But the water-resisting strata are relatively thin and usually damaged by the geological structures, such as faults and collapse columns. Furthermore, the water-resisting strata may break under the combined action of hydraulic and mining-induced pressures during coal mining above the aquifer. And a dramatic increase in permeability may occur in the broken water-resisting floor strata and finally result in water bursting into mining excavations [5, 6]. Water inrush hazard not only leads to grievous casualties and heavy economic losses for coal mines but also seriously pose a potential threat to society stability [7–14]. According to incomplete official statistics, about 285 major coalmines involve a risk of water inrush in China, which approximately accounts for 47.5% of all state-owned coalmines [15]. And more than 473 water inrush hazards have occurred in the past two decades killing 2635 workers [16]. Therefore, the study of prediction and prevention on floor water inrush has important practical significance.

In recent decades, many researches on floor water inrush mechanism have been conducted. A few empirical criteria and models, such as the water inrush index, hypothesis of three zones in floor strata, and floor key strata model, have been proposed for predicting water inrushes [1, 14, 17–21]. These studies played an important role in evaluating the risk of water inrush hazards in engineering practice. However, there is a lack of methods to accurately predict and prevent water inrush hazards in a timely manner [22]. This has limited our ability to address the crucial issue for safer

mining above confined aquifers. After coal mining, the redistribution of stress field may result in a fractured zone with high conductivity in the floor strata, which provides a pathway for confined water inflow [23–25].

In general, the formation of water inrush pathway is directly related to the fracture of floor rock strata, which induces a series of microseismic to occur [26]. Currently, microseismic has been widely used to monitor the rock failure process in landslide, coal and gas outbursts, and coal bumps and predict these hazards [27–31]. However, microseismic was seldom applied to monitor the formation process of water inrush pathway, which is a requirement of water inrush. In this article, the mechanics criteria of floor water inrush are derived based on cusp catastrophe theory and the criteria are utilized to assess floor water inrush risk in the Ruifeng coalmine. Floor water inrush is more likely to occur during mining because the geological structures are complex in the study area. Therefore, ESG microseismic monitoring system was applied to monitor the formation process of water inrush pathway, which provides an important guide for the prevention of water inrush. The field monitoring results show that two water inrush pathways were accurately positioned. Then, two targeted grouting holes were drilled from the ground surface and the water inrush was effectively prevented by injecting 900 tons of cement slurry. This provides significant guidance for safe coal excavation above confined aquifers.

2. General Situation of the Study Area

Ruifeng coalmine located in Handan-Xingtai mining area of North China is severely threatened by water inrush hazards. In Handan-Xingtai mining area, more than 10 collieries involve the risk of water bursting into the mining excavation through fractured floor strata and more than 30 heavy water inrush hazards occurred in the past, as shown in Figure 1 and Table 1. The main influencing factors causing water inrush are collapse columns, faults, and mining. As can be seen from Figure 1 and Table 1, 14 water inrush hazards were caused by faults which accounted for forty-seven percent and 11 water inrush hazards were caused by collapse columns which accounted for thirty-seven percent. Besides, 2 water inrush hazards were caused by the combined action of faults and collapse columns and other 2 water inrush hazards were caused by floor failure due to mining. Furthermore, the most serious water inrush accident occurred on April 12, 2003 in the Dongpang coalmine and the maximum water inrush rate was 70000 m^3/h, which caused the coalmine to submerge, and there were a large number of casualties. Therefore, geological structures, mainly including insidious faults and collapse columns, are the main influencing factors of water inrush in Handan-Xingtai mining area.

In the Ruifeng coalmine, there are Ordovician limestone strata under the No. 5 coal seam, which contains a large amount of water with a 1.33~1.73 MPa pressure. The average thickness of No. 5 coal seam is about 8.0 m and is located in the level at a depth of −460 m. The distance between Ordovician limestone strata and No. 5 coal seam is about 49 m. More than 30 collapse columns have been exposed during the past mining. There are three main faults and two collapse columns in the study area, as shown in Figure 1. Besides, a total of 17 water inrush hazards have occurred in the past. The most serious water inrush occurred in 1942 and the maximum water inrush rate was about 4080 m^3/h, causing the coalmine to submerge in half an hour.

3. Risk Assessment of Floor Water Inrush Based on the Cusp Catastrophe Theory

In order to reduce floor water inrush hazards, the vulnerability assessment of floor aquifuge is necessary [32, 33]. The roof caving did not occur behind the mining face within a certain range. Therefore, the unloading failure of floor aquifuge happens, which may cause floor water inrush.

Simplifying the unbroken floor aquifuge as a rock beam, as shown in Figure 2, the length of the rock beam is equal to the length of the mining face. The width of the rock beam is the unit length and the thickness of the rock beam can be calculated by the following formula [34]:

$$h_2 = h - h_1, \tag{1}$$

where h_2 is the thickness of the rock beam, h is the thickness of floor aquifuge, and h_1 is the depth of floor failure zone due to mining activities, which can be determined by the following empirical formula:

$$h_1 = \frac{0.015H\cos\varphi}{2\cos(\pi/4+\varphi/2)}e^{(\pi/4+\varphi/2)\tan\varphi}, \tag{2}$$

where H is the buried depth of the coal seam and φ is the internal friction angle.

Based on the definition of the elastic strain energy and the beam bending theory, the elastic strain energy U can be calculated by the following formula [35]:

$$U = \frac{EI}{2}\int_0^L k^2 \mathrm{d}s, \tag{3}$$

where s is the arc length between the original point of the beam and the arbitrary point, k is the curvature of the rock beam. Due to $\omega' << 1$, therefore the curvature k can be approximately written as follows:

$$k = \frac{\omega''}{\left(1+\omega'^2\right)^{3/2}} \approx \omega''\left(1+\omega'^2\right)^{1/2}, \tag{4}$$

where ω is the deflection of the arbitrary point, which can be defined as follows:

$$\omega \approx \delta \sin\frac{\pi}{L}s, \tag{5}$$

where L is the length of the beam and δ is the deflection of the beam midpoint.

Substituting equations (4) and (5) into equation (3), the elastic strain energy U can be written as follows:

$$U \approx \frac{EI}{2}\int_0^L \omega''^2\left(1+\omega'^2\right)\mathrm{d}s = \frac{EI\pi^6\delta^4}{16L^5} + \frac{EI\pi^4\delta^2}{4L^3}, \tag{6}$$

where $I = {h_2}^3/12$.

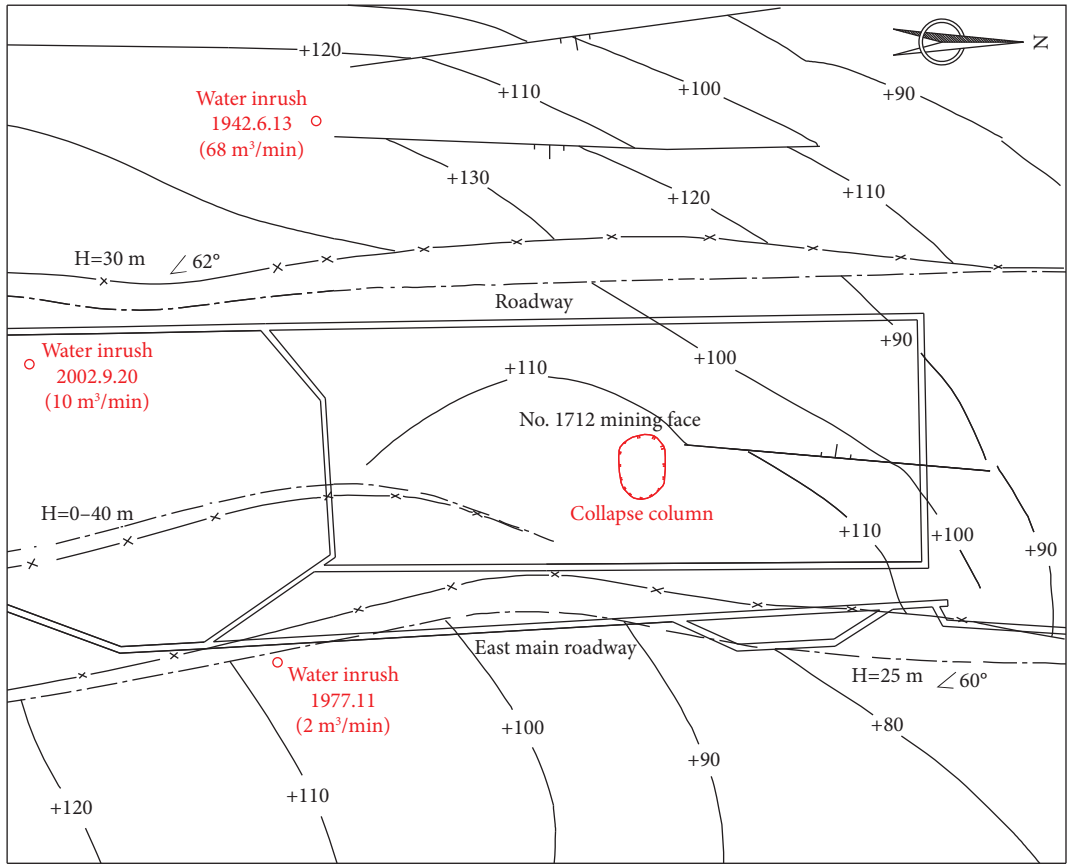

Figure 1: Geological structures in the study area of the Ruifeng coalmine.

The work done W_1 by the horizontal forces can be expressed as follows:

$$W_1 = \sigma_3 h_2, \Delta L = \sigma_3 h_2 \left(L - \int_0^L \sqrt{1 - \omega'^2}\, \mathrm{d}s \right), \tag{7}$$

where ΔL is the horizontal shortened length of the beam because of the action of horizontal force.

Utilizing Taylor series expansion and ignoring the higher order term, we can get the following equation:

$$\sqrt{1 - \omega'^2} \approx 1 - \frac{\omega'^2}{2}. \tag{8}$$

Substituting equation (8) into equation (7), W_1 can be written as follows:

$$W_1 \approx \frac{\sigma_3 h_2}{2} \int_0^L \omega'^2 \mathrm{d}s = \frac{\sigma_3 h_2 \pi^2 \delta^2}{4L}. \tag{9}$$

Likewise, the work done W_2 by vertical forces can be represented as follows:

$$W_2 = \int_0^L (p - q)\omega \mathrm{d}s = \frac{2(p - q)L}{\pi}\delta, \tag{10}$$

where $q = \gamma h_1$.

The behaviour of a system is usually continuous, but sometimes exhibits discontinuities, which needs to be studied by bifurcation or catastrophe theory. Based on Thom's classification theorem, there are seven elementary catastrophes, where the number of state variables is one or two and the number of control parameters (equal to the codimension) is four. One of the simple catastrophes is cusp catastrophe which involves two control parameters and one state variable. The maxima, minima, and inflection points of the potential function are known as stationary points. These points may be a singularity at which the value of the potential function can jump [36]. Therefore, the potential function should be established first. According to the catastrophe theory, the total potential energy V of the beam can be written as follows:

$$V = U - W_1 - W_2. \tag{11}$$

Substituting equations (6), (9), and (10) into equation (11), the total potential energy V can be approximated as follows:

$$V \approx \frac{EI\pi^6}{16L^5}\delta^4 + \frac{\pi^2}{4L}\left(\frac{EI\pi^2}{L^2} - \sigma_3 h_2 \right)\delta^2 - \frac{2(p - q)L}{\pi}\delta. \tag{12}$$

Equation (12) is the steady-state model of the rock beam and can be further transformed as the following standard form [35]:

$$V = x^4 + ax^2 + bx, \tag{13}$$

where

Table 1: Incomplete statistics of serious water inrush hazards in Handan-Xingtai mining area.

Number	Coal mine	Date	Maximum water inrush rate (m^3/h)	Water inrush types
1	Wutongzhuang	1995-12-3	34000	Fault
2	Wutongzhuang	2001-3-10	156	Collapse column
3	Wutongzhuang	2002-6-7	480	Fault
4	Wutongzhuang	2002-3-21	120	Fault
5	Wutongzhuang	2000-5-14	130	Collapse column
6	Wutongzhuang	2006-1-26	3900	Fault
7	Wutongzhuang	2014-7-25	11250	Collapse column
8	Huangsha	2010-11-19	6000	Fault
9	Huangsha	2011-12-11	24000	Fault and collapse column
10	Huangsha	1996-12-19	1320	Mining activities
11	Huangsha	2010-11-19	6000	Fault
12	Jiulong	2009-1-8	7200	Collapse column
13	Jiulong	2007-9-29	5400	Collapse column
14	Jiulong	2007-10-21	720	Collapse column
15	Jiulong	2009-1-1	900	Collapse column
16	Jiulong	2009-1-11	7200	Collapse column
17	Xin'an	2010-11-19	6000	Fault
18	Xin'an	2011-12-11	24000	Collapse column
19	Xin'an	2011-12-11	2600	Fault and collapse column
20	Ruifeng	2002-9-20	600	Fault
21	Ruifeng	1977-11	120	Collapse column
22	Ruifeng	1932-8	480	Fault
23	Ruifeng	1942-6-13	4080	Fault
24	Dongpang	2003-4-12	70000	Collapse column
25	Dongpang	2010-11-15	2500	Mining activities
26	Niuerzhuang	2004-9-26	5160	Fault
27	Sunzhuang	1996-11-24	9000	Fault
28	Xingdong	2011-4-13	330	Mining activities
29	Shenjiazhuang	2012-5-26	740	Fault
30	Lincheng	2006-12-16	3600	Fault

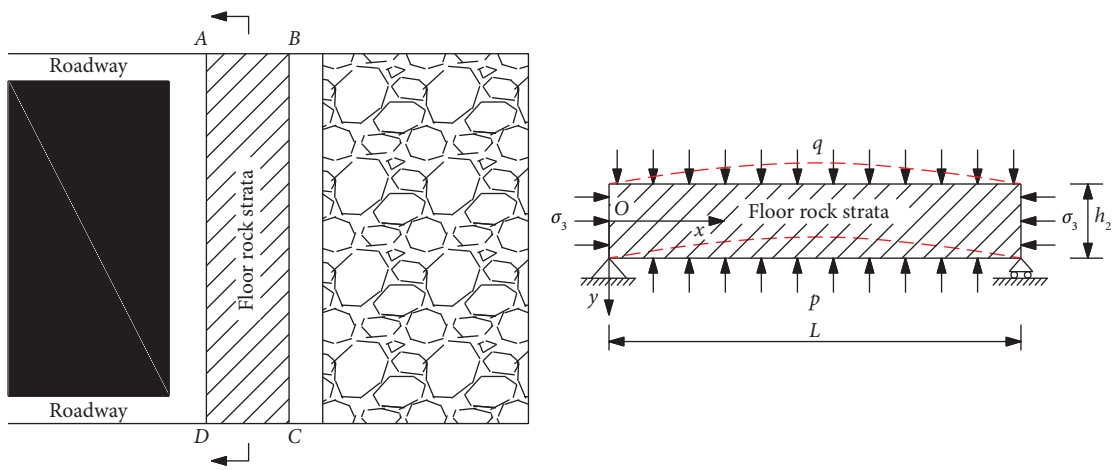

Figure 2: The simplified mechanical model of floor aquifuge.

$$x = \frac{\pi}{2L}\sqrt[4]{\frac{EI\pi^2}{L}}\delta,$$

$$a = L\sqrt{\frac{L}{EI\pi^2}}\left(\frac{EI\pi^2}{L^2} - \sigma_3 h_2\right), \quad (14)$$

$$b = -\frac{4(p-q)L^2}{\pi^2}\sqrt[4]{\frac{L}{EI\pi^2}}.$$

The discriminant of floor water inrush is as follows [35]:

$$\Delta = 8a^3 + 27b^2 \begin{cases} > 0 & \text{no water inrush,} \\ = 0 & \text{critical state,} \\ < 0 & \text{water inrush.} \end{cases} \quad (15)$$

The system potential energy of rock beam is minimum when $\Delta > 0$. Therefore, the rock beam is stable and the water inrush cannot occur. However, it is on the contrary when $\Delta < 0$, namely, the rock beam is unstable and the water inrush occurs. When $\Delta = 0$, it is in critical state and the floor water inrush may occur under minimal engineering disturbance. In the Ruifeng coalmine, the hydraulic pressure of the confined aquifer is $p \approx 1.33 \sim 1.73$ MPa and the thickness of the aquifuge is $h \approx 49.0$ m. The buried depth of the No.5 coal seam is about −460 m and the internal friction angle of the floor aquifuge is about 30°. Taking the above parameters to equation (2), the depth of floor failure zone due to mining activities is about $h_1 \approx 12$ m. Besides, relevant physical and mechanical parameters are as follows: $L \approx 80$ m, $E \approx 10$ GPa, $h_2 \approx 37$ m, $q \approx 0.5$ MPa, and $\sigma_3 \approx 11.5$ MPa, and taking the above parameters to equation (15), we can get $\Delta > 0$. In other words, the floor aquifuge is stable and mining above confined aquifer is safe. But considering the complex geological structures such as faults and collapse columns in the study area, floor water inrush still may occur during mining. Therefore, ESG microseismic monitoring system was applied to monitor the formation of water inrush pathway, which can predict floor water inrush.

4. Numerical Analysis on Floor Water Inrush in the Ruifeng Coalmine

Floor water inrushes can be classified into two types: geological structures-controlled water inrush and mining-induced water inrush. The former is mainly caused by faults and karst collapse columns in the floor strata [37–39], the latter is directly related to the mining activities [3, 5, 22]. Mining activities would damage the floor aquifuge causing a decrease of aquifuge thickness. When the thickness of aquifuge decreases to the limit value, a water inrush accident must happen. Furthermore, mining makes the shear stress on the fault plane increase, which may cause the activation of faults and provide a pathway for confined water inflow. In the following, the software FLAC^{3D} [40] was applied to simulate the plastic zone evolution of floor aquifuge containing a collapse column and the evolution of shear stress on fault plane when the mining face advances to the geological structures.

4.1. Collapse Column. In this section, the software FLAC^{3D} was applied to simulate the plastic zone evolution of floor aquifuge with the mining face advances to the collapse column. The numerical model is built based on the geological data of the Ruifeng coalmine. The numerical model is 250 m long, 160 m wide, and 180 m high. The horizontal section of collapse column is ellipse and its geometric parameters are shown in Figure 3. The physical and mechanical parameters of coal and rock strata are obtained based on experimental results, as shown in Table 2.

The depth of plastic zone of floor strata caused by mining is proportional to the mining thickness of the coal seam. Stress field and plastic zone around the collapse column are also influenced by mining activities. In the numerical simulation, the mining face begins with 80m from the collapse column. The mining face advanced 30, 60, 75, 80, 85, 100, 130, and 160 m, respectively, with the distance of the mining face at 80 m, 50 m, 20 m, and 5 m before the center of the collapse column and −5 m, −20 m, −50 m, and −80 m after the center of the collapse column. Figure4 shows the plastic zone evolution when the mining thickness is 2 m, 4 m, 6 m, and 8 m, respectively.

In general, the rock masses would undergo plastic yield when the tension stress or shear stress reach the limit value. The shear stress of floor aquifuge would increase at mining face after coal excavation. Furthermore, the peak value of shear stress increases as the mining thickness increases. The shear stress concentration would increase the range of floor plastic zone as shown in Figure 5. Before the mining face reaches the collapse column (mining advance less than 75 m), the plastic zone around the collapse column does not change. However, when the mining face reaches the collapse column, the plastic zone above the collapse column spread upward because of shear stress concentration. The depth of floor plastic zone is about 2.0 m, 4.0 m, 8.0 m, and 12.0 m when the mining thickness is 2.0 m, 4.0 m, 6.0 m, and 8.0 m, respectively. Furthermore, when the mining thickness is less than 6.0 m, the floor shallow plastic zone does not connect to the plastic zone around the collapse column. However, when the mining thickness is 8.0 m, the floor shallow plastic zone connects to the deep plastic zone, which indicates that the floor water inrush may occur. Therefore, the mining thickness has important influence on floor water inrush. In order to avoid floor water inrush accident and realize safe mining, the mining thickness should be less than 6.0 m.

4.2. Fault. The direct stress along the normal fault is tensile stress, which makes the cracks of tension-crushed zone open and connected. The floor water stored in the aquifer is more likely to flow through the aquifuge along the fault. Therefore, floor water inrush may occur when the mining face advances to the fault. Besides, the strength of the rock is very low near the fault plane, where the rocks fail more easily due to abutment pressure caused by mining activities. And this may result in a larger failure zone and increase the water inrush

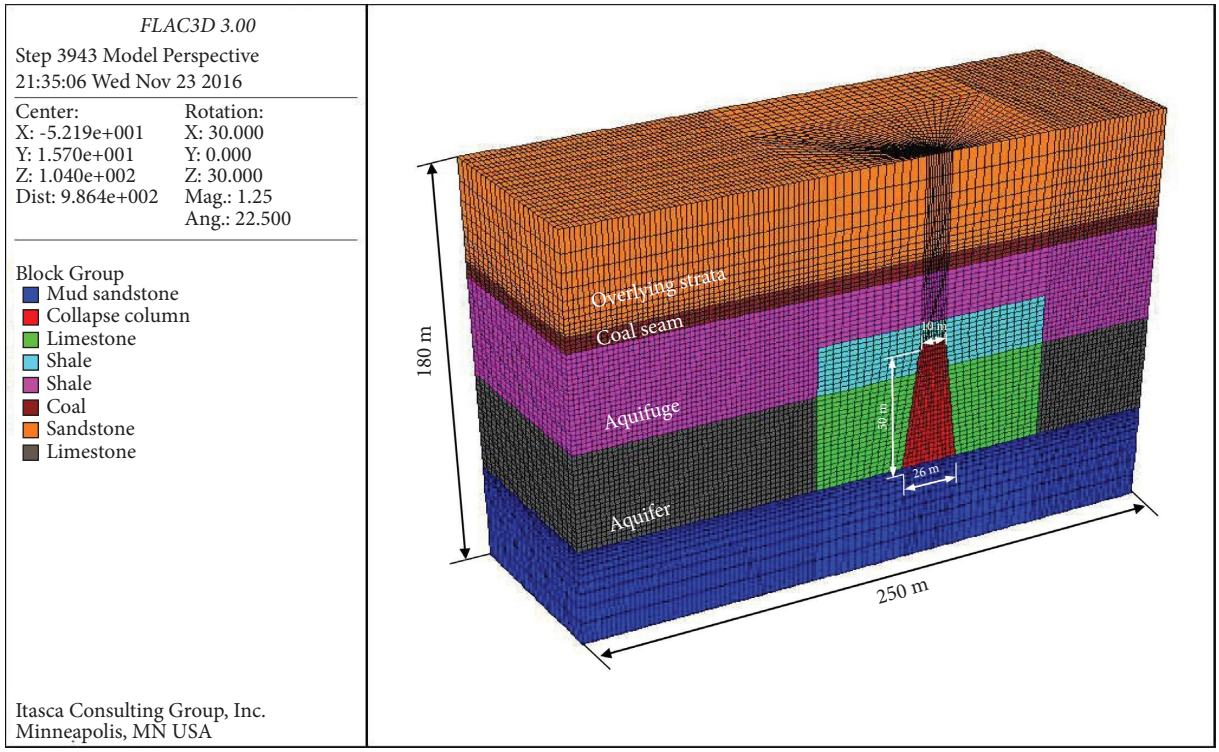

Figure 3: The numerical model of floor water inrush caused by collapse column.

Table 2: Physical and mechanical parameters of coal and rock.

Strata	Density (10^3 kg/m^3)	Elastic modulus (GPa)	Poisson's ratio	Internal friction angle (°)	Cohesion (MPa)	Tensile strength (MPa)
Sandy mudstone	2.60	25.92	0.26	30	9.13	1.45
Limestone	2.53	29.45	0.15	31	16.25	3.79
Shale	2.61	34.30	0.18	34	20.00	3.00
Coal	2.49	34.59	0.20	33	15.00	3.70
Sandstone	2.50	36.70	0.16	32	14.40	2.69

quantity. The numerical model is 250 m long, 120 m wide, and 160 m high. The monitoring points on the fault plane are located at −5 m, −10 m, −15 m, −20 m, −25 m, −30 m, −35 m, −40 m, and −45 m, as shown in Figure 4. The physical and mechanical parameters of coal and rock strata are shown in Table 3.

Shear stress on the fault plane usually plays an important role in the fault activation. Figure 6 shows the variation laws of shear stress on fault plane when the mining face advances to the fault. It can be seen from Figure 7 that the shear stress on fault plane increases at first and then decreases before the mining face reaches the fault. After the mining face reaches the fault, the shear stress decreases at first and finally reaches stable. With the mining face advancing to the fault, the deep shear stress of fault plane increases at first and then the shallow shear stress of fault plane increases. Furthermore, the shear stress on fault plane in shallow floor is more influenced by mining. The maximum shear stress is 9.7 MPa and the maximum shear stress concentration factor is about 1.9. The shear stress peaks when the mining face is about 20 m away from the fault, the fault is more likely to slide causing floor water inrush; but after the mining face reaches the fault, mining has small influence on the shear stress on the fault plane.

5. Judgment of Floor Water Inrush Based on Microseismic Monitoring Results

5.1. Microseismic Monitoring Floor Water Inrush and the Layout of ESG Sensors. The geological conditions are very complex in the study area because there are many faults and collapse columns. Floor water inrush is very difficult to accurately position and predict by the traditional methods. However, coal mining causes breakage of the floor aquifuge, which is accompanied by acoustic emission [41, 42]. Microseismic monitoring system could capture the AE information and position the fractured zone of floor strata, which is a necessary condition for floor water inrush. The analysis procedure of floor water inrush based on microseismic monitoring is shown in Figure 7. The floor water inrush pathway can be achieved by the spatial distribution of microseismic events. All ESG sensors are mainly installed in the east main roadway and No. 3050 return air lane, as shown in Figure 8. The positional parameters of ESG sensors

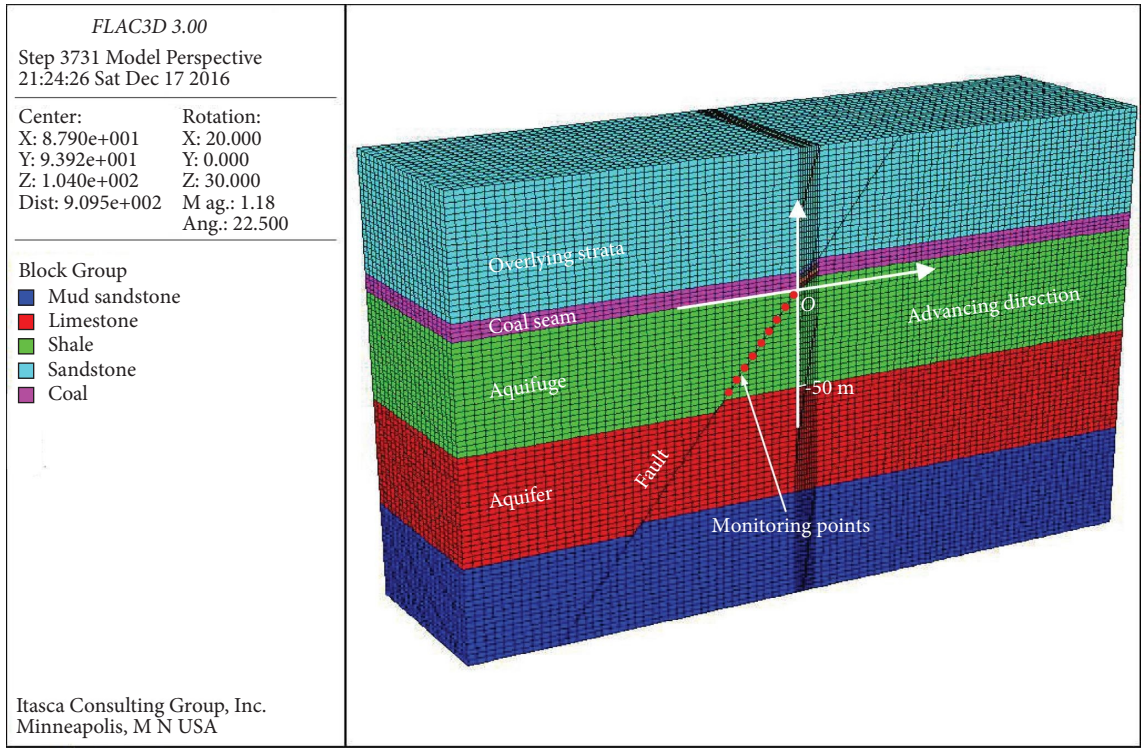

Figure 4: The numerical model of floor water inrush caused by the fault.

are shown in Table 3. The ESG sensors include 9 single pathway sensors (no. 1, no. 3, no. 4, no. 6, no. 7, no. 8, no. 9, no. 11, and no. 12) and 3 three-pathway sensors (no. 2, no. 5, and no. 10).

5.2. Microseismic Monitoring Results. The variation of energy release index and accumulated volume are shown in Figure 9. It was significantly found that a sharp increase of the energy release index occurred and the accumulated volume decreased suddenly on February 25, when the floor water inrush occurred. The floor aquifuge might experience the dynamic process that "energy accumulation ⟶ energy release ⟶ energy transfer," matches well with the monitoring results of energy release index and accumulated volume. Therefore, floor water inrush is closely related to the variation of energy release index and accumulated volume. A sudden sharp change of energy release index or accumulated volume may be precursory characteristics of floor water inrush.

About 500 microseismic events occurred during the nearly four months' monitoring and the spatial distribution of microseismic events is shown in Figure 10. The size of red dots represents the magnitude of microseismic events, namely, the bigger dot means that the rock fractures more seriously. As shown in Figure 11, the microseismic events initially occurred in the Ordovician limestone because of confined water. Besides, the floor strata unload after coal excavation, which causes the failure of the shallow floor aquifuge. Therefore, some microseismic events occurred in the shallow floor strata. Under the combined action of mining and confined water, the shallow floor fractured zone finally connected to the aquifer and caused floor water inrush. There are two obvious water inrush pathways, located near two faults separately. One water inrush pathway is along the fault and the other water inrush pathway intersects the fault. Finally, the two water inrush pathways intersected at the water inrush position. The range of water inrush pathway gradually increases, which may cause the increase of water inrush rate.

6. Targeted Grouting to Prevent Floor Water Inrush

In the Ruifeng coalmine, the traditional method to prevent floor water inrush is pregrouting, namely, some holes were drilled from the roadways into floor aquifuge and grouting cement slurry was conducted ahead of the mining face, as shown in Figure 11. Two grouting holes with different dip angle and length were drilled at the same place in the roadway. The average apace between two adjacent grouting positions was about 40 meters. If the traditional pregrouting method was used, 52 grouting holes need to be drilled and the total length of grouting holes is about 3640 meters long. Furthermore, about 7600 tons of cement slurry would be injected.

But previous field practice show that the traditional pregrouting method was less effective to prevent floor water inrush and the cost was very high, because the grouting area was very large and the grouting holes were drilled blindly. Therefore, to effectively prevent floor water inrush and reduce the cost, targeted grouting method was proposed based on microseismic monitoring

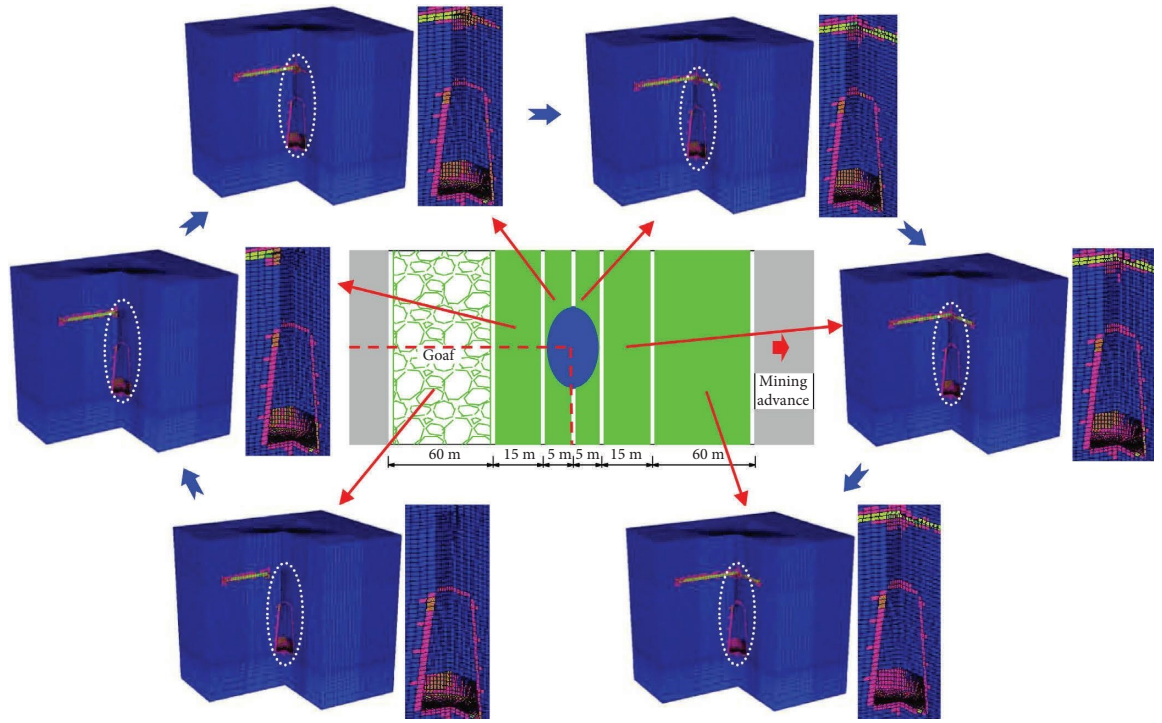

(a)

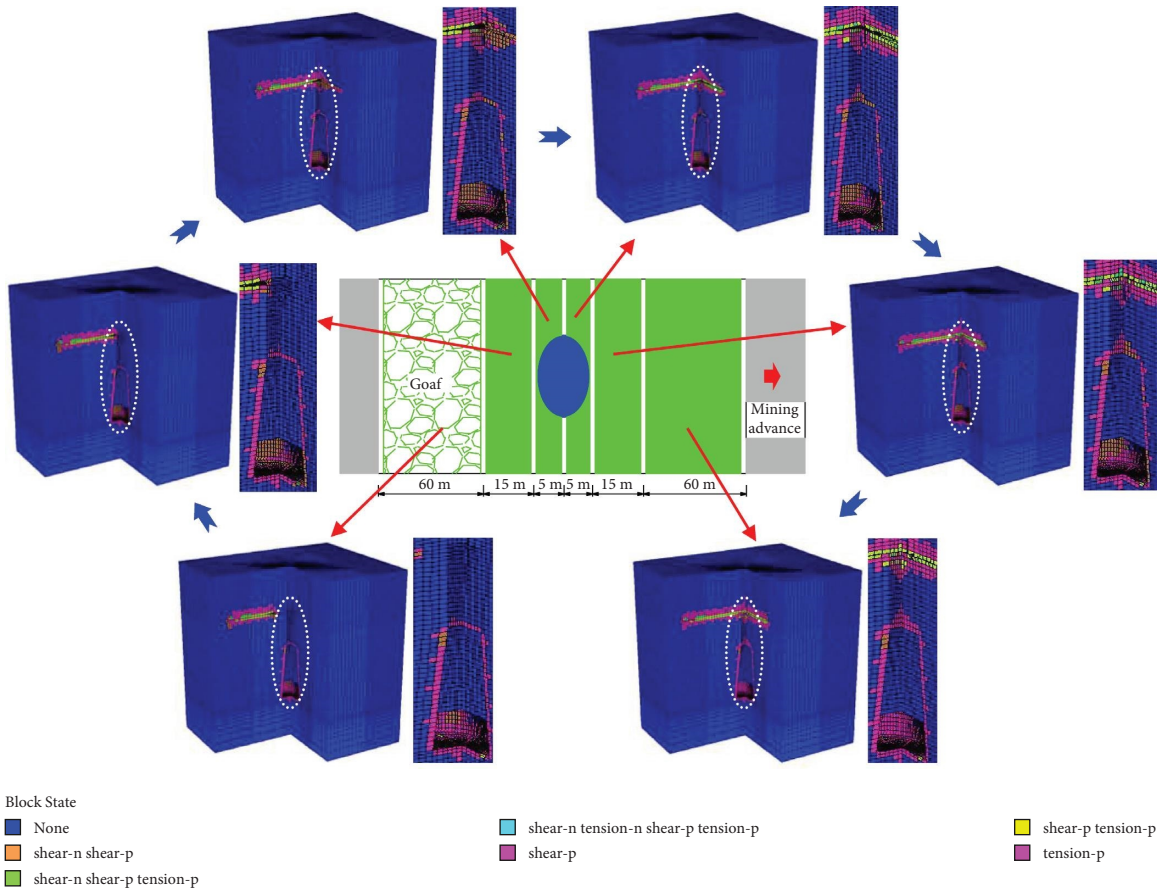

(b)

Figure 5: Continued.

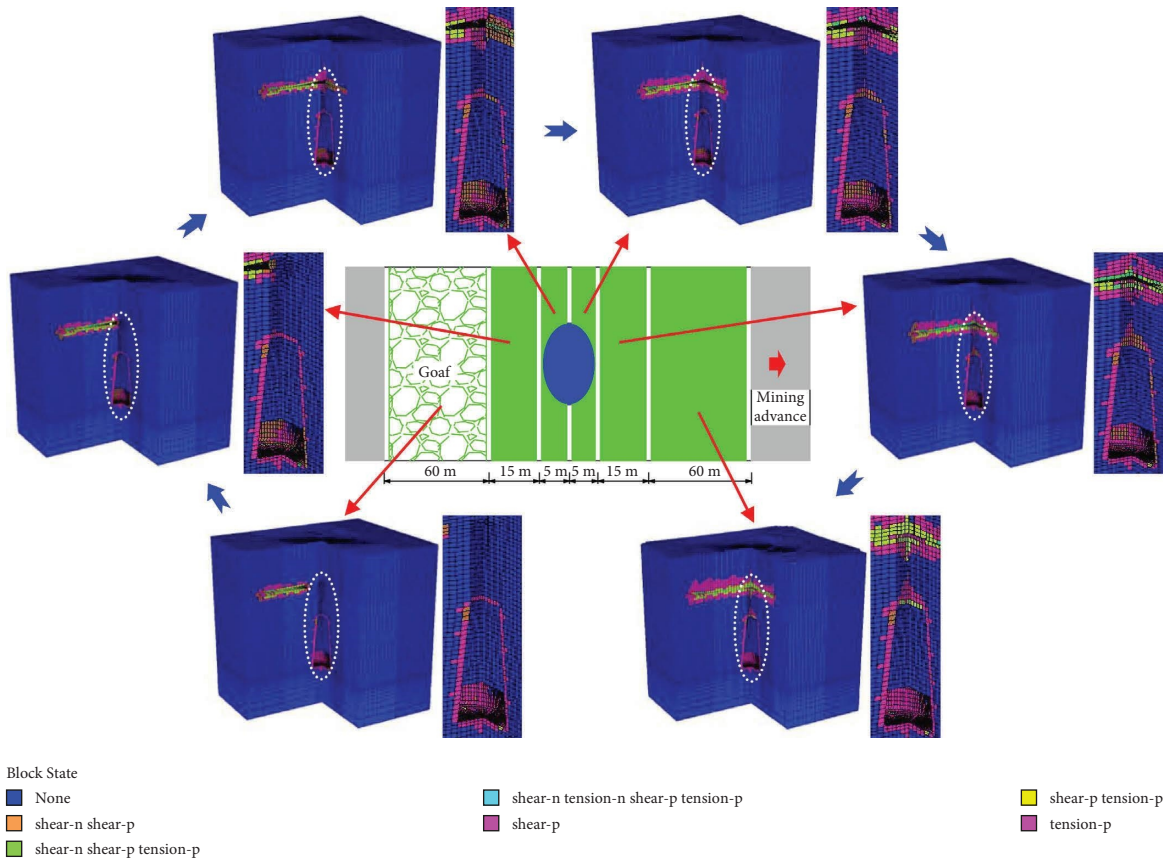

(c)

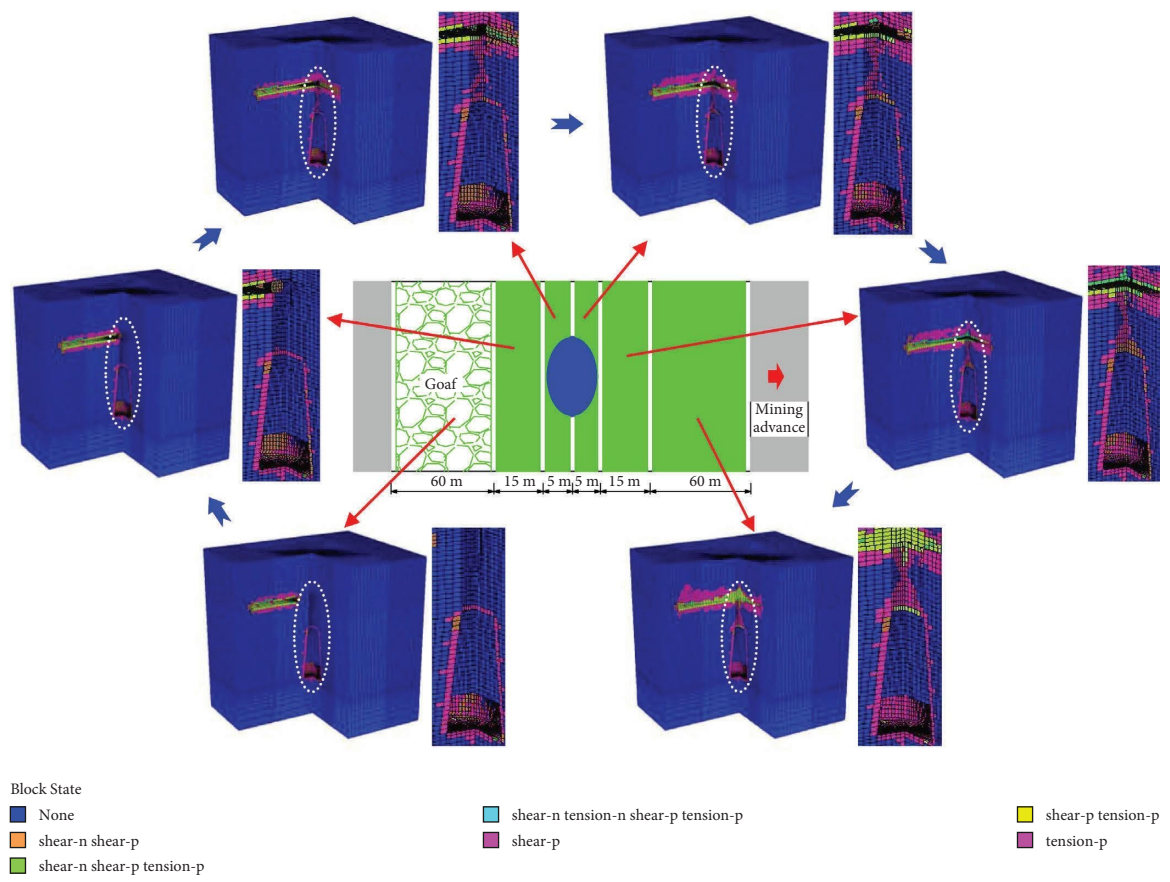

(d)

Figure 5: The damage zone evolution of floor strata during mining. (a) The mining thickness is 2 m; (b) the mining thickness is 4 m; (c) the mining thickness is 6 m; and (d) the mining thickness is 8 m.

Table 3: The positional parameters of ESG sensors in the Ruifeng coalmine.

Number	The coordinates of ESG sensors			Dip angle (°)	Azimuthal angle (°)
	X	Y	Z		
1#	12395.492	20588.497	132.706	−30	−1
2#	12396.375	20505.893	132.185	−3	−2
3#	12429.610	20453.61	145.646	−30	88
4#	12509.072	20451.167	151.798	0	88
6#	12668.078	20462.936	144.475	0	179
5#	12588.771	20449.825	146.475	25	89
7#	12377.051	20634.143	132.239	−10	−93
8#	12464.329	20629.132	132.639	30	−93
10#	12633.068	20619.294	134.876	−25	−93
9#	12555.178	20624.009	133.174	30	−93
11#	12704.326	20614.977	134.877	0	−93
12#	12778.648	20623.827	134.882	−15	−94

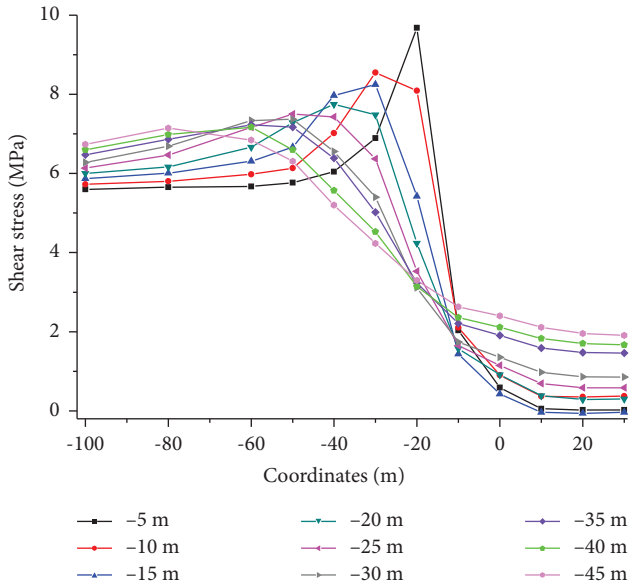

Figure 6: The variation laws of shear stress on the fault plane when the mining face advances to the fault.

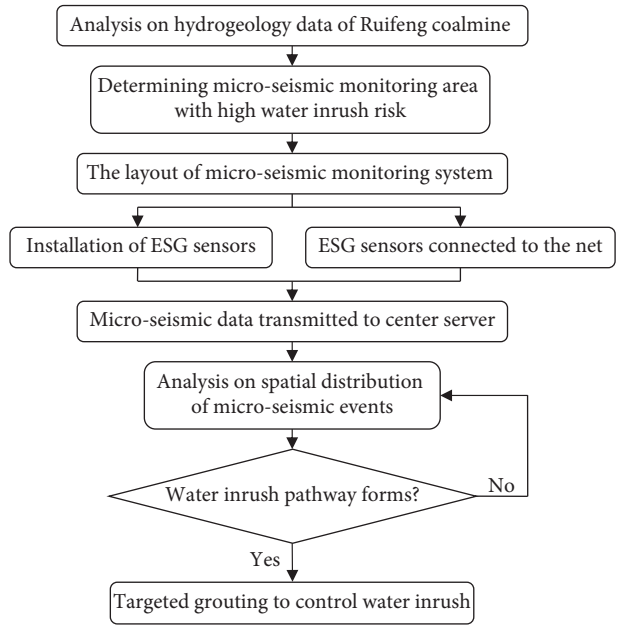

Figure 7: The procedure of floor water inrush control based on microseismic monitoring in the Ruifeng coalmine.

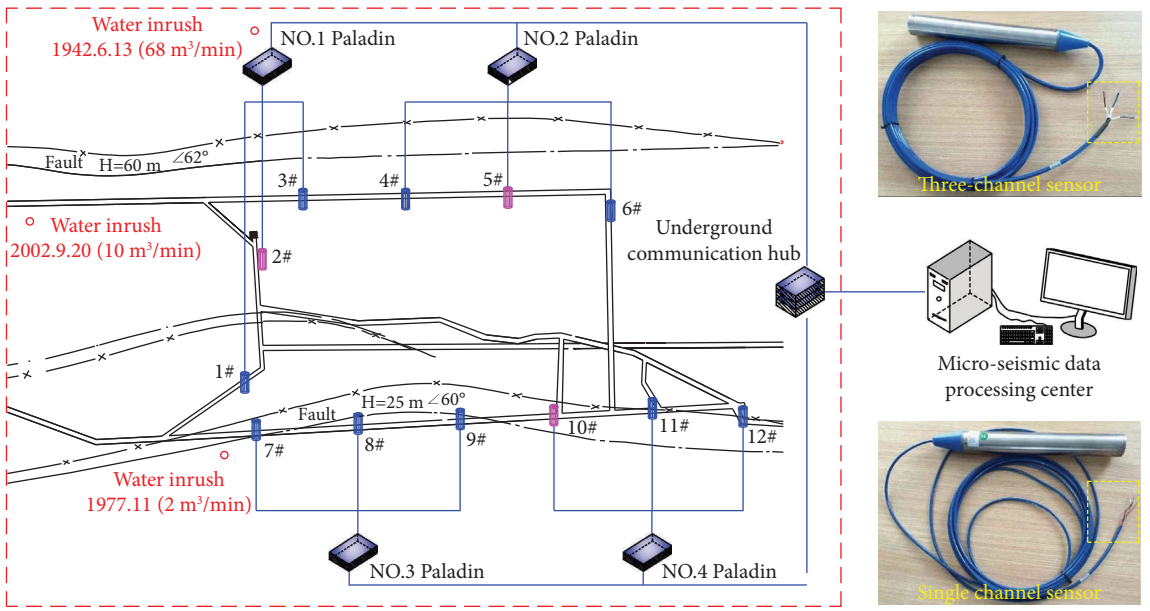

Figure 8: The layout of ESG sensors in the Ruifeng coalmine.

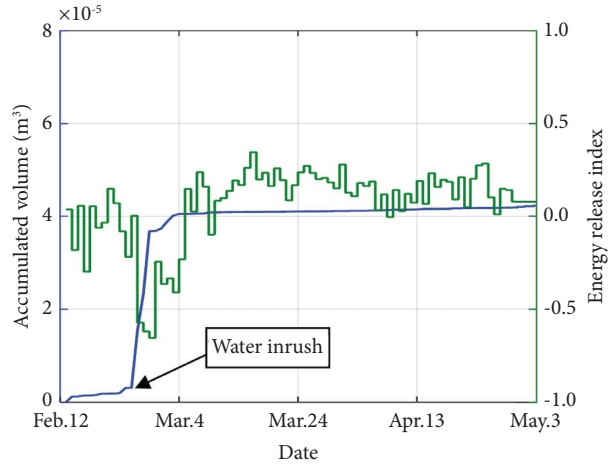

Figure 9: The variation laws of energy release index and accumulated volume.

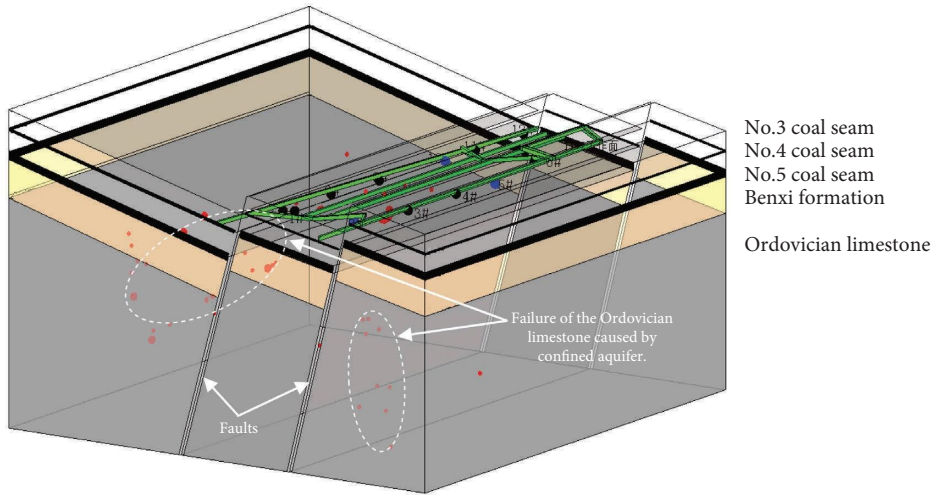

(a)

Figure 10: Continued.

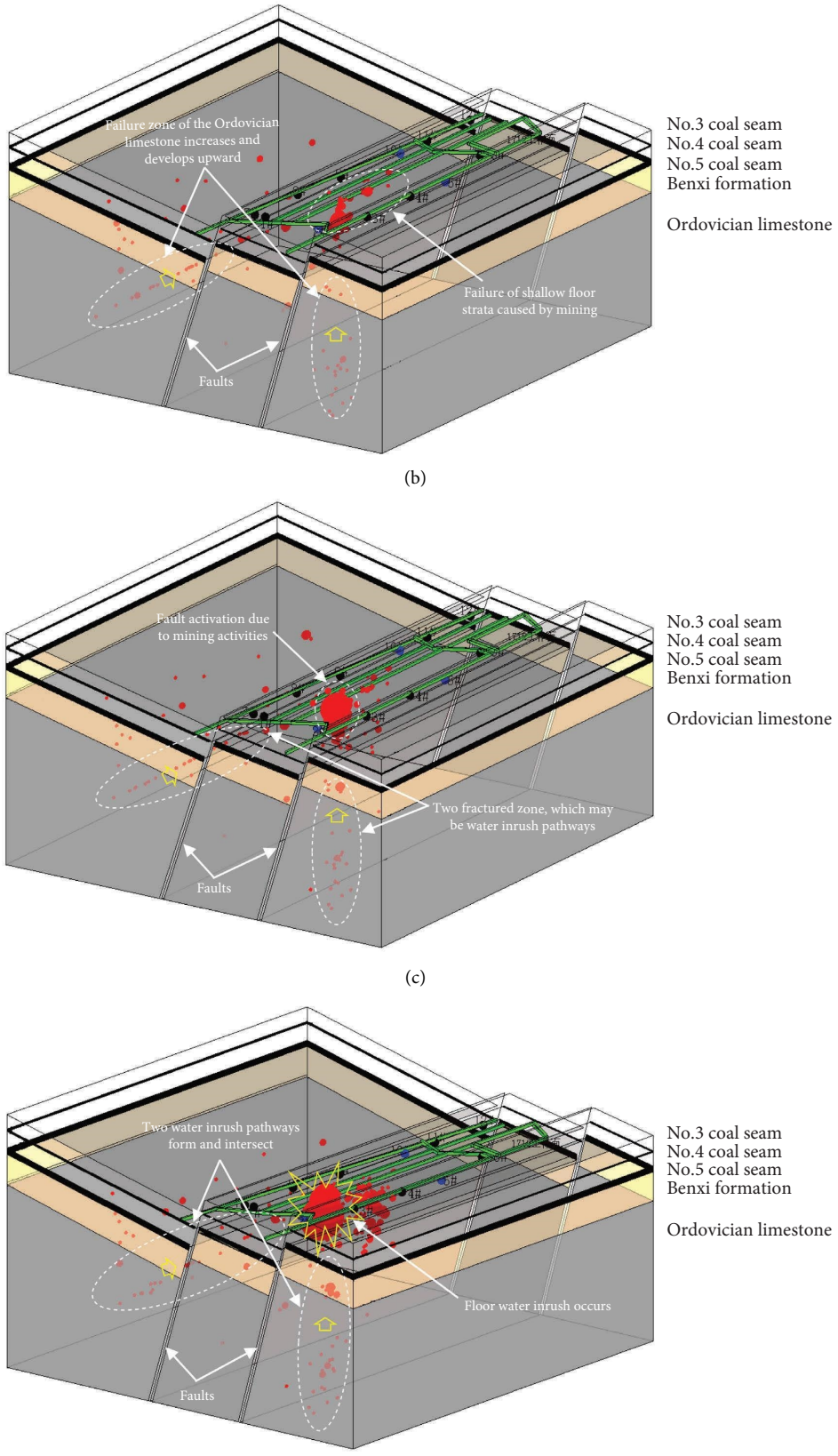

Figure 10: Continued.

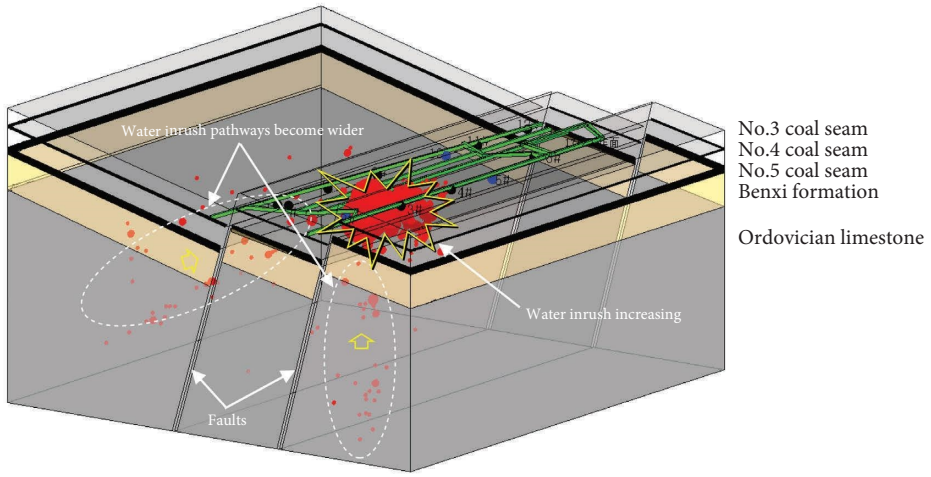

(e)

Figure 10: Spatial distribution of microseismic events in the Ruifeng coalmine.

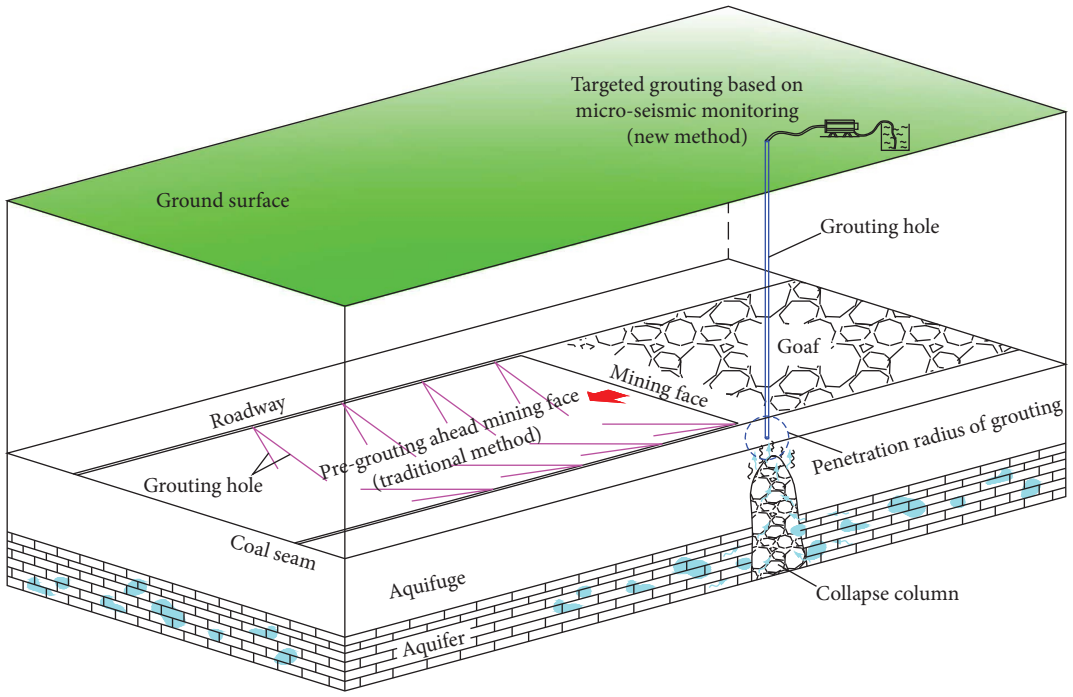

Figure 11: The pregrouting method and targeted grouting method to prevent floor water inrush in the Ruifeng coalmine.

results, as shown in Figure 11. Two water inrush pathways were positioned based on microseismic monitoring system. Correspondingly, two targeted grouting holes can be drilled from the ground. The total length of two grouting holes is about 950 meters, which is much less than that of the traditional pregrouting method. Furthermore, the water inrush was effectively prevented by injecting 900 tons of cement slurry, which was only a quarter of what the traditional pregrouting method consumed. Therefore, the targeted grouting method is more effective to prevent water inrush and significantly reduces the cost.

The variation laws of grouting pressure, water inflow rate, and microseismic events are shown in Figure 12. The water inrush occurred on February 25 and the targeted grouting was conducted 5 days later. The initial grouting pressure was 1.0 MPa and the final grouting pressure was 3.0 MPa. There are some fluctuations of grouting pressure because of the permeability change of floor strata. Additionally, the water inrush rate dramatically decreased from 80 m^3/h to 20 m^3/h after grouting for three days. In the end, the floor water inrush was completely prevented after grouting for 40 d. During the initial period of grouting, the

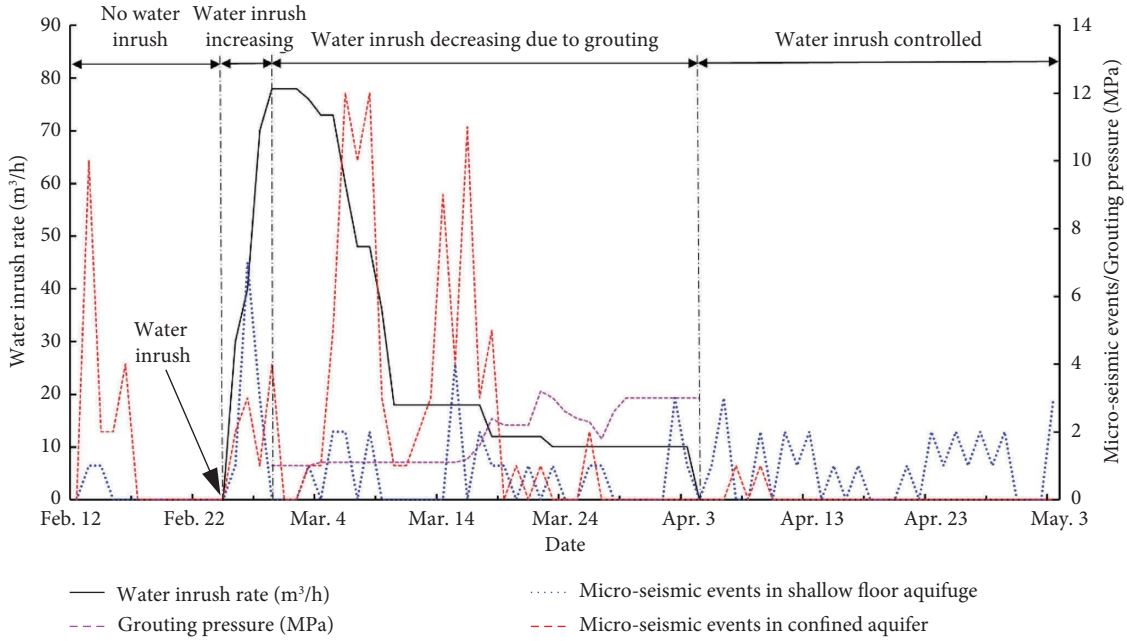

Figure 12: Variation laws of grouting pressure, water inrush rate, and microseismic events.

microseismic events still occurred in Ordovician limestone due to hydraulic fracturing. There are almost no microseismic events in Ordovician limestone after stopping grouting. But a few microseismic events in shallow floor strata occurred all the time due to mining activities.

7. Conclusions

(1) Water inrush is the biggest threat for safe mining in the Ruifeng coalmine and the floor water inrush were mainly caused by mining activities and geological structures in the study mining area. Floor water inrush is more likely to occur during mining because the geological structures are complex in the study area. Based on cusp catastrophe theory, the mechanics criteria of floor water inrush is derived and the criteria is utilized to assess floor water inrush risk of the Ruifeng coalmine.

(2) The failure process of the floor aquifuge during mining is achieved by numerical simulating. The mining thickness has important influence on floor water inrush. The depth of floor plastic zone increases with the increase of mining thickness. When the mining thickness is less than 6.0 m, the floor shallow plastic zone does not connect to the plastic zone around the collapse column. However, when the mining thickness is 8.0 m, the floor shallow plastic zone connects to the deep plastic zone, which indicates that the floor water inrush may occur. Therefore, in order to avoid floor water inrush, the mining thickness should be less than 6.0 m.

(3) The shear stress on the fault plane increases at first and then decreases before the mining face reaches the fault. After the mining face reaches the fault, the shear stress decreases at first and finally reaches stable. With the mining face advancing to the fault, the deep shear stress of the fault plane increases at first and then the shallow shear stress of the fault plane increases. Furthermore, the shear stress on the fault plane in shallow floor is more influenced by mining. The shear stress peaks when the mining face is about 20 m away from the fault, where the fault is more likely to slide causing floor water inrush.

(4) ESG microseismic monitoring system was applied to monitor the formation process of water inrush pathway. The field monitoring results show that two water inrush pathways were accurately positioned. Then, two grouting holes were drilled from the ground surface and the water inrush was effectively prevented by injecting 900 tons of cement slurry, which significantly reduced the cost.

Data Availability

The proposed numerical model and data used during the current study are available from the corresponding author.

Conflicts of Interest

The authors declare that they have no conflicts of interest.

Acknowledgments

This work was supported by the China Postdoctoral Science Foundation (no. 2020M680756).

References

[1] J. C. Zhang, "Investigations of water inrushes from aquifers under coal seams," *International Journal of Rock Mechanics and Mining Sciences*, vol. 42, no. 3, pp. 350–360, 2005.

[2] Q. Wu, M. Wang, and X. Wu, "Investigations of groundwater bursting into coal mine seam floors from fault zones," *International Journal of Rock Mechanics and Mining Sciences*, vol. 41, no. 4, pp. 557–571, 2004.

[3] J. A. Wang and H. Park, "Coal mining above a confined aquifer," *International Journal of Rock Mechanics and Mining Sciences*, vol. 40, no. 4, pp. 537–551, 2003.

[4] Y. L. Lu and L. G. Wang, "Numerical simulation of mining-induced fracture evolution and water flow in coal seam floor above a confined aquifer," *Computers and Geotechnics*, vol. 67, pp. 157–171, 2015.

[5] J. A. Wang and H. Park, "Fluid permeability of sedimentary rocks in a complete stress–strain process," *Engineering Geology*, vol. 63, no. 3-4, pp. 291–300, 2002.

[6] W. Q. Liu, X. D. Fei, and J. N. Fang, "Rules for confidence intervals of permeability coefficients for water flow in over-broken rock mass," *International Journal of Mining Science and Technology*, vol. 22, no. 1, pp. 29–33, 2012.

[7] Q. Wang, B. Jiang, S. Xu et al., "Roof-cutting and energy-absorbing method for dynamic disaster control in deep coal mine," *International Journal of Rock Mechanics and Mining Sciences*, vol. 158, Article ID 105186, 2022.

[8] Q. Wang, S. Xu, Z. X. Xin, M. C. He, H. Y. Wei, and B. Jiang, "Mechanical properties and field application of constant resistance energy-absorbing anchor cable," *Tunnelling and Underground Space Technology*, vol. 125, Article ID 104526, 2022.

[9] S. B. Tang, J. M. Li, S. Ding, and L. T. Zhang, "The influence of water-stress loading sequences on the creep behavior of granite," *Bulletin of Engineering Geology and the Environment*, vol. 81, no. 11, p. 482, 2022.

[10] W. C. Zhu and C. H. Wei, "Numerical simulation on mining-induced water inrushes related to geologic structures using a damage-based hydromechanical model," *Environmental Earth Sciences*, vol. 62, no. 1, pp. 43–54, 2011.

[11] Q. Wu and W. Zhou, "Prediction of groundwater inrush into coal mines from aquifers underlying the coal seams in China: vulnerability index method and its construction," *Environmental Geology*, vol. 56, no. 2, pp. 245–254, 2008.

[12] G. Li and W. Zhou, "Impact of karst water on coal mining in North China," *Environmental Geology*, vol. 49, no. 3, pp. 449–457, 2006.

[13] T. Glade and F. Nadim, "Early warning systems for natural hazards and risks," *Natural Hazards*, vol. 70, no. 3, pp. 1669–1671, 2014.

[14] J. C. Zhang and B. H. Shen, "Coal mining under aquifers in China: a case study," *International Journal of Rock Mechanics and Mining Sciences*, vol. 41, no. 4, pp. 629–639, 2004.

[15] W. Q. Peng, W. J. Wang, and Q. F. Li, "Reasonable width of waterproof coal pillar under the condition of different fault dip angles," *Journal of Mining and Safety Engineering*, vol. 26, no. 2, pp. 179–186, 2009.

[16] Z. P. Meng, R. Wang, Y. Y. Wang, J. Liu, J. H. Zhang, and J. Yuan, "Geologic evaluation of water inrush risk for No.12 coal seam floor of Fangezhuang mine field in Kailuan," *Journal of Mining and Safety Engineering*, vol. 27, no. 3, pp. 310–315, 2010.

[17] X. Liang, S. B. Tang, C. A. Tang, L. H. Hu, and F. Chen, "Influence of water on the mechanical properties and failure behaviors of sandstone under triaxial compression," *Rock Mechanics and Rock Engineering*, vol. 56, no. 2, pp. 1131–1162, 2022.

[18] Y. J. Sun, J. P. Zuo, M. Karakus, and J. T. Wang, "Investigation of movement and damage of integral overburden during shallow coal seam mining," *International Journal of Rock Mechanics and Mining Sciences*, vol. 117, pp. 63–75, 2019.

[19] R. Zhang, Z. Q. Jiang, H. Y. Zhou, C. W. Yang, and S. J. Xiao, "Groundwater outbursts from faults above a confined aquifer in the coal mining," *Natural Hazards*, vol. 71, no. 3, pp. 1861–1872, 2014.

[20] J. P. Zuo, S. P. Peng, Y. J. Li, Z. H. Chen, and H. P. Xie, "Investigation of karst collapse based on 3-D seismic technique and DDA method at Xieqiao coal mine, China," *International Journal of Coal Geology*, vol. 78, no. 4, pp. 276–287, 2009.

[21] Y. Wang, C. Zhu, M. C. He, X. Wang, and H. L. Le, "Macro-meso dynamic fracture behaviors of Xinjiang marble exposed to freeze thaw and frequent impact disturbance loads: a lab-scale testing," *Geomechanics and Geophysics for Geo-Energy and Geo-Resources*, vol. 8, no. 5, p. 154, 2022.

[22] T. H. Yang, J. S. Liu, W. C. Zhu, D. Elsworth, L. G. Tham, and C. A. Tang, "A coupled flow– stress–damage model for groundwater outbursts from an underlying aquifer into mining excavations," *International Journal of Rock Mechanics and Mining Sciences*, vol. 44, no. 1, pp. 87–97, 2007.

[23] S. Levasseur, R. Charlier, B. Frieg, and F. Collin, "Hydro-mechanical modelling of the excavation damaged zone around an underground excavation at Mont Terri Rock Laboratory," *International Journal of Rock Mechanics and Mining Sciences*, vol. 47, no. 3, pp. 414–425, 2010.

[24] Y. J. Sun, J. P. Zuo, M. Karakus, L. Liu, H. W. Zhou, and M. L. Yu, "A new theoretical method to predict strata movement and surface subsidence due to inclined coal seam mining," *Rock Mechanics and Rock Engineering*, vol. 54, no. 6, pp. 2723–2740, 2021.

[25] W. C. Zhu and O. T. Bruhns, "Simulating excavation damaged zone around a circular opening under hydromechanical conditions," *International Journal of Rock Mechanics and Mining Sciences*, vol. 45, no. 5, pp. 815–830, 2008.

[26] K. Katsuyama, *Applications of Acoustic Emission (AE) Techniques*, China Metallurgical Industry Press, Beijing, China, 1997.

[27] N. W. Xu, C. A. Tang, L. C. Li et al., "Micro-seismic monitoring and stability analysis of the left bank slope in Jinping first stage hydropower station in southwestern China," *International Journal of Rock Mechanics and Mining Sciences*, vol. 48, no. 6, pp. 950–963, 2011.

[28] V. L. Shkuratnik, L. Filimonov, and S. V. Kuchurin, "Regularities of acoustic emission in coal samples under triaxial compression," *Journal of Mining Science*, vol. 41, no. 1, pp. 44–52, 2005.

[29] J. Li, S. C. Wu, Y. T. Gao, L. Li, and Y. Zhou, "An improved multidirectional velocity model for micro-seismic monitoring in rock engineering," *Journal of Central South University*, vol. 22, no. 6, pp. 2348–2358, 2015.

[30] C. L. Wang, "Identification of early-warning key point for rock mass instability using acoustic emission/microseismic activity monitoring," *International Journal of Rock Mechanics and Mining Sciences*, vol. 71, pp. 171–175, 2014.

[31] C. Zhu, Y. Z. Xu, Y. X. Wu et al., "A hybrid artifi cial bee colony algorithm and support vector machine for predicting blast-induced ground vibration," *Earthquake Engineering and Engineering Vibration*, vol. 21, no. 4, pp. 861–876, 2022.

[32] S. Fuchs, J. Birkmann, and T. Glade, "Vulnerability assessment in natural hazard and risk analysis: current approaches and future challenges," *Natural Hazards*, vol. 64, no. 3, pp. 1969–1975, 2012.

[33] B. Schwendtner, M. Papathoma-Köhle, and T. Glade, "Risk evolution: how can changes in the built environment influence the potential loss of natural hazards," *Natural Hazards and Earth System Sciences*, vol. 13, no. 9, pp. 2195–2207, 2013.

[34] S. X. Yin, J. C. Zhang, and D. M. Liu, "A study of mine water inrushes by measurements of in situ stress and rock failures," *Natural Hazards*, vol. 79, no. 3, pp. 1961–1979, 2015.

[35] D. X. Liang, Z. Q. Jiang, S. Y. Zhu, Q. Sun, and Z. W. Qian, "Experimental research on water inrush in tunnel construction," *Natural Hazards*, vol. 81, no. 1, pp. 467–480, 2015.

[36] X. R. Wang, K. Guan, T. H. Yang, and X. G. Liu, "Instability mechanism of pillar burst in asymmetric mining based on cusp catastrophe model," *Rock Mechanics and Rock Engineering*, vol. 54, no. 3, pp. 1463–1479, 2021.

[37] L. Lianchong, Y. Tianhong, L. Zhengzhao, Z. Wancheng, and T. Chunan, "Numerical investigation of groundwater outbursts near faults in underground coal mines," *International Journal of Coal Geology*, vol. 85, no. 3-4, pp. 276–288, 2011.

[38] C. Neuzil and J. V. Tracy, "Flow through fractures," *Water Resources Research*, vol. 17, no. 1, pp. 191–199, 1981.

[39] R. Zimmerman and G. Bodvarsson, "Effective transmissivity of two-dimensional fracture networks," *International Journal of Rock Mechanics and Mining Sciences & Geomechanics Abstracts*, vol. 33, p. 433, 1996.

[40] Itasca, *Fast Lagrangian Analysis of Continua in 3 Dimensions Manual*, Itasca Consulting Group Inc, Minneapolis, MN, USA, 2015.

[41] D. P. Jansen, S. R. Carlson, R. P. Young, and D. A. Hutchins, "Ultrasonic imaging and acoustic emission monitoring of thermally induced micro cracks in Lac du Bonnet Granite," *Journal of Geophysical Research: Solid Earth*, vol. 98, no. B12, pp. 22231–22243, 1993.

[42] C. Li and E. Nordlund, "Experimental verification of the Kaiser effect in rocks," *Rock Mechanics and Rock Engineering*, vol. 26, no. 4, pp. 333–351, 1993.